High Island Densities and Long Range Repulsive Interactions: Fe on Epitaxial Graphene

S. M. Binz,[1] M. Hupalo,[1] Xiaojie Liu,[1,2] C. Z. Wang,[1] Wen-Cai Lu,[2,3] P. A. Thiel,[4] K. M. Ho,[1]
E. H. Conrad,[5] and M. C. Tringides[1]

[1]*Ames Laboratory–U.S. Department of Energy, and Department of Physics and Astronomy, Iowa State University,
Ames, Iowa 50011, USA*
[2]*State Key Laboratory of Theoretical and Computational Chemistry, Institute of Theoretical Chemistry, Jilin University,
Changchun, Jilin 130021, People's Republic of China*
[3]*College of Physics and Laboratory of Fiber Materials and Modern Textile, the Growing Base for State Key Laboratory,
Qingdao University, Qingdao, Shandong 266071, People's Republic of China*
[4]*Ames Laboratory–U.S. Department of Energy, Department of Chemistry and Department of Materials Science and Engineering,
Iowa State University, Ames, Iowa 50011, USA*
[5]*School of Physics, Georgia Institute of Technology, Atlanta, Georgia 30332, USA*

The understanding of metal nucleation on graphene is essential for promising future applications, especially of magnetic metals which can be used in spintronics or computer storage media. A common method to study the grown morphology is to measure the nucleated island density n as a function of growth parameters. Surprisingly, the growth of Fe on graphene is found to be unusual because it does not follow classical nucleation: n is unexpectedtly high, it increases continuously with the deposited amount θ and shows no temperature dependence. These unusual results indicate the presence of long range repulsive interactions. Kinetic Monte Carlo simulations and density functional theory calculations support this conclusion. In addition to answering an outstanding question in epitaxial growth, i.e., to find systems where long range interactions are present, the high density of magnetic islands, tunable with θ, is of interest for nanomagnetism applications.

Understanding the growth of metals on graphene is essential for many potential graphene applications [1–6]. Metals will be used as contacts for graphene-based devices so it is important to minimize the electrical resistance [7–9], which requires finding conditions for the metal to grow layer by layer. Metals are used to dope graphene and control the number of carriers for microelectronics applications [10], so it is essential for the charge transfer between metal and carbon atoms to be weak, so the unique graphene electronic structure is not distorted. Magnetic metals grown on graphene [11–14] can be used in computer storage devices if a high island density can be grown in a controlled way, and as spin filters if smooth graphene layers can be sandwiched between magnetic metal films. All these promising applications are based on finding ways to understand and control the grown metal morphology.

Direct information about the metal growth and the metal graphene interaction can be obtained by imaging the growth outcome with STM. An easily measurable quantity the nucleated island density n and its dependence on growth parameters (temperature, flux rate, coverage) has been the standard method to collect the information carried out in many epitaxial systems [15]. After deposition, n is analyzed to extract the key controlling barriers like the terrace diffusion barrier E_D and cohesive energy E_i of the 2D islands. In classical nucleation [15] n determines the diffusion coefficient $D = D_0 \exp(-E_D/k_B T)$: low n implies fast diffusion while high n indicates slow diffusion.

$$D = F\left(\frac{\eta \exp(E_i/(i_c + 2)k_B T)}{n}\right)^{(i_c + 2/i_c)}, \quad (1)$$

where F is the flux rate and i_c is the critical size cluster (i.e., the minimum number of deposited adatoms necessary so the nucleated island is stable). No adatom-adatom interactions are included in this analysis. It has been predicted that if such interactions are present and are also long range and repulsive, high, tunable and spatially correlated island densities, with weak temperature dependence are possible. It has been a challenge to find experimental systems where long range interactions are present; finding such interactions in metal graphene systems can lead to more rational and predictive growth.

For practically all metals grown on graphene [16,17] the coverage θ dependence of n followed classical nucleation attaining steady state at low deposited amounts when the surface area covered is approximately 5%. The constant n at steady state is determined by the condition that the diffusion length becomes equal to the decreasing island separation. However, for Fe growth on graphene an unusual behavior was found, with n increasing continuously with θ and surprisingly with very weak T dependence. This unusual result signifies the presence of long range repulsive interactions between the Fe adatoms, that suppresses with increasing θ the aggregation of the Fe adatoms to preexisting islands. The magnitude of the repulsive interactions can be extracted from the comparison of the experimental images

with kinetic Monte Carlo simulations modeling growth with long range interactions, which were calculated with density-functional theory (DFT) [18–20]. The Fe experiments show how to produce high density of magnetic islands and how this density becomes controllable (by 4 orders of magnitude from 10^{-6} to 10^{-2} islands/nm^2) simply by tuning the deposited Fe amount.

The experiments were carried out with a variable temperature Omicron STM. The method of preparing graphene is described in Refs. [17,21]. Graphene is grown after thermal annealing of $6H$-SiC(0001) and a highly homogeneous sample is prepared with predominantly (85%) single layer graphene. The homogeneity of the sample can be seen in images in Refs. [17,21]. Standard tests were applied to distinguish single from bilayer graphene (from the voltage dependence of the buried interface of the buffer layer $6\text{-}\sqrt{3} \times \sqrt{3}$ and step height differences between single and bilayer graphene). An Omicron molecular-beam epitaxy source was used for Fe deposition and the flux rate was measured from the ion current which is a constant fraction of the flux rate. The flux rate was further verified from the integrated volume of the deposited islands.

The deviation of the Fe nucleation from the standard expectations is seen in Fig. 1. For room temperature deposition, n continues to increase even up to 2.3 ML (55% covered area because the nucleated islands are 3D) and possibly beyond. A continually rising n requires a steady nucleation of new islands, which are seen in the form of small islands in Figs. 1(b)–1(f). θ is varied over 3 orders of magnitude from 0.002 to 2.3 ML. It is remarkable that for very low θ indeed a very low n is observed (with these initial Fe islands still 3D and containing several hundred atoms). This shows that initially the diffusion length is at least 50 nm [the average island separation in Fig. 1(b)], since the large number of deposited atoms incorporated in the islands must traverse such large distances. However, as more Fe atoms are deposited [see Figs. 1(c)–1(f)] the diffusion length must continuously decrease while n correspondingly increases.

Figure 2(a) shows the dependence of n on the deposition temperature T from 300 to 650 K. Despite the large temperature change $\Delta T = 350$ K, the island density is almost constant and fluctuates around its mean value $\sim 6 \times 10^{-4}$ islands/nm^2 by less than a factor of 2. This is a very weak temperature dependence and not consistent with activated thermal diffusion [16]. In Figs. 2(b)–2(d) θ is ~ 0.6 ML and in Fig. 2(e) it is 1.05 ML. On the other hand for Fe/Fe(001) at 300 K [22] n is 6×10^{-3} islands/nm^2 at RT dropping to 10^{-3} islands/nm^2 at 550 K. Nucleation theory [15] was used to extract the diffusion barrier $E_d = 0.45$ eV and normal prefactor $\nu_0 \sim 10^{12}$ hops/s.

Figure 3 gives more detailed information about island heights and sizes. New islands nucleate, as close as 5 nm to existing islands. Three different size islands, large, medium, and small, are clearly seen from typical line scans, indicating the different times of the ongoing nucleation processes. The large islands do not exceed lateral size of 7 nm. The islands have curved tops because of tip convolution. A fraction (40%) of newly arriving Fe atoms diffuses to the large islands and moves to higher layers, while a larger fraction (60%) nucleates new islands. The diffusion length measured at the lower $\theta = 0.003$ ML is at least 10 times larger than 5 nm, the average distance from preexisting islands at which new islands nucleate. So apparently there is a barrier that prohibits the adatoms to attach to the islands already present. Encountering another
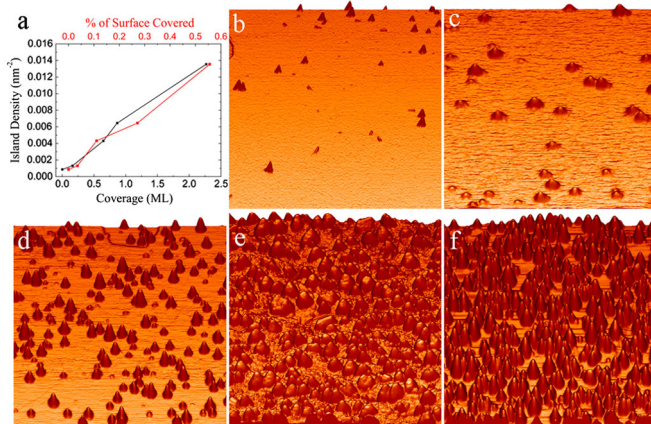

FIG. 1 (color online).   (a) Island density n vs θ for Fe grown on graphene at room temperature showing a monotonic dependence on θ up to at least 55% surface coverage ($\theta = 2.3$ ML). (b)–(f) Corresponding images at different θ; (b) 0.003 ML, (c) 0.16 ML, (d) 0.65 ML, (e) 0.87 ML, and (f) 2.3 ML. Small islands in each image show the new islands that have just nucleated. All images are 200×200 nm^2 except (c) which is 150×150 nm^2.
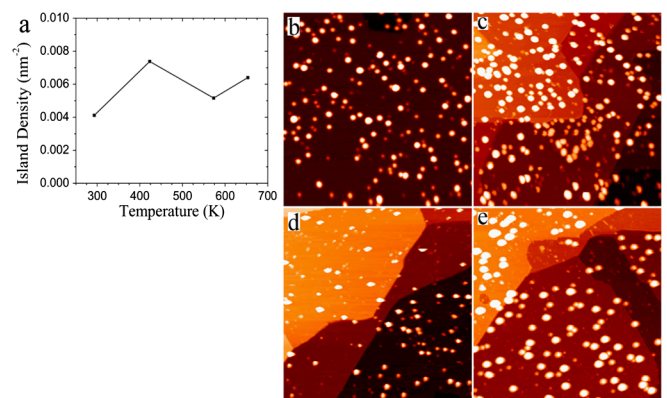

FIG. 2 (color online).   (a) Temperature dependence of the island density n from 300 to 650 K. The temperatures and coverages are (b) RT, 0.65 ML, (c) 420 K, 0.65 ML, (d) 570 K, 0.54 ML, and (e) 650 K, 1.05 ML. Classical nucleation predicts an Arrhenius dependence of n with temperature while images (b)–(e) instead show an almost constant island density. Each image is 200×200 nm^2.
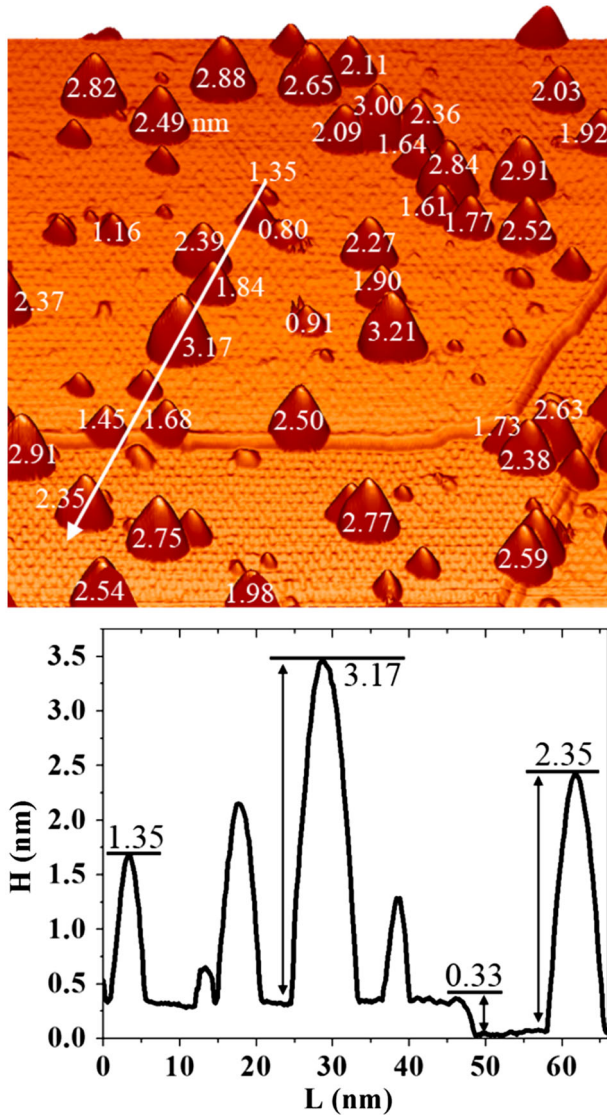
FIG. 3 (color online). A detailed image of the structure and distribution of Fe islands. The area is 100×100 nm^2 $n = 7 \times 10^{-3}$ islands/nm^2, $\theta = 0.6$ M, $T = 450$ K, and $F = 9 \times 10^{-4}$ ML/sec. New islands nucleate at a distance as close as 5 nm to preexisting islands. Three different size islands are seen from the image and the line scan. The larger islands are 15 layer high. The 6-$\sqrt{3} \times \sqrt{3}$ is visible between the islands.

diffusing adatom, that was also repelled, results in the nucleation of a new island, so the island density continues to grow with θ.

This intuitive expectation is supported quantitatively from DFT calculations and Monte Carlo simulations in the literature, performed to determine the role of long range interactions in nucleation. Such simulations have been carried out to understand homoepitaxy in several metal-metal systems [Ag/Ag(111), Cu/Cu(111)] which have low diffusion barriers and very low diffusion prefactors [18–20]. This work has shown that repulsive interactions

can dramatically increase n (when compared to the case of no interactions), can lead to increasing n with θ, to a much weaker dependence of n on T and can account for the measured low prefactors. Although the origin of these interactions was mediated through the metallic substrate and most likely is different from the origin of the interactions for Fe on graphene, the effects on nucleation are similar.

The interactions between two adatoms separated by distance s with s less than 6 lattice constants were calculated with DFT in Refs. [18–20]. These interactions were implemented (additively and in pairwise fashion), in kinetic Monte Carlo simulations to model island nucleation, irrespectively of the local environment of the two adatoms. The repulsive interaction $\Delta E_d(s) > 0$ was added to the total barrier experienced by an incoming adatom ($E_d + \Delta E_d$) so the probability of the diffusing adatom to approach the second adatom a distance s away was reduced by $p(s) = \exp - (\Delta E_d(s)/k_B T)$. Instead of using the barriers E_d, ΔE_d, it is more useful for the comparison with Fe on graphene, to use the ratios D/F and to quantify the strength of the repulsive interactions in terms of the smallest probability $p(s) = p_{\min}$. The latter is the key parameter that captures the reduced probability to aggregate to preexisting islands and therefore to increase n.

In Ref. [18] the D/F ratios were in the range $E_d/kT = 15$, $4 \times 10^6 > D/F > 5 \times 10^5$, with $p_{\min} = 1.5 \times 10^{-2}$ and n was found to increase by 2 orders of magnitude and to become temperature independent. In Ref. [19] the temperature was even lower $E_d/kT = 23$ but a similar ratio was obtained for the relaxed surface $D/F = 10^5$ and $p_{\min} = 1.5 \times 10^{-2}$ as in Ref. [18]. Besides the simulations a mean field theory was applied for nucleation with long range interactions in Ref. [20] with similar range $7 \times 10^5 < D/F < 5 \times 10^{11}$ and $\Delta E_d(s)$ as in Ref. [19]. It gave a similar increase for n by 2 orders of magnitude when compared to the case of no interactions. These simulations lead to at least two robust conclusions: (i) pairwise additive interactions up to $s = 6$ can have very dramatic effect on n (ii) $p_{\min} \approx 2 \times 10^{-2}$ is more than sufficient for n to be dramatically different from what expected by classical theory of nucleation (and to show similar behavior as in Figs. 1 and 2).

How are these kinetic Monet Carlo results applied to Fe on graphene? Using the relevant parameters for Fe on graphene $E_d = 0.5$ eV (this is a low bound to the terrace diffusion barrier as discussed in [16]) $F = 9 \times 10^{-4}$ ML/s, $T = 300$ K–700 K, $\nu_0 = 10^{12}$ s^{-1} we deduce $6 \times 10^{10} > D/F > 3 \times 10^7$ similar to the ratios [18–20]. Since the deviations from standard nucleation are comparable to the ones simulated in Refs. [18–20] $p_{\min} = 2 \times 10^{-2}$ can account for these results. This value of $p_{\min}$ implies a maximum barrier $\Delta E_d = 0.1$ eV at the lowest temperature 300 K. Is this estimate of the maximum ΔE_d reasonable?
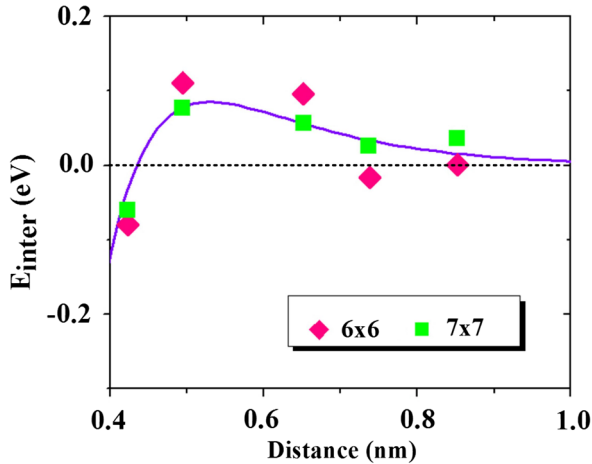
PHYSICAL REVIEW LETTERS

FIG. 4 (color online). DFT calculated interaction energy between two Fe adatoms $E_{inter}(s)$ as a function of s. The interaction is attractive at small s but becomes repulsive at $s > 0.5$ nm with the barrier $\Delta E_d = 0.1$ eV and $p_{min} = 10^{-2}$ at 300 K.

Similar to the work in [18–20], the interactions between two adatoms on graphene were calculated by DFT with generalized gradient approximation in the form of PBE [23] implemented in the VASP code, including spin polarization and dipole moment corrections [17,24]. Valence electrons were treated explicitly and their interactions with ionic cores were described by projector augmented wave pseudopotentials The dimension of the supercell in the z direction is 1.5 nm which allows a vacuum region of about 1.2 nm to separate the atoms and their replicas in the z direction. The supercell dimensions were kept fixed during the relaxation. Although the exact DFT method and whether van der Waals terms are included in the calculations can affect the theoretical results in some systems [25], the excellent agreement between measured and calculated diffusion and adsorption barriers [17,24] justifies the theoretical approximation used for the current calculations.

The interaction energy is defined as $E_{inter}(s) = E_{a2}(s)-2E_{a1}$ where $E_{a2}(s)$ is the adsorption energy of two Fe adatoms on graphene at separation s and E_{a1} is the adsorption energy of a single Fe adatom. Figure 4 shows $E_{inter}(s)$ as a function of s. The Fe-Fe interaction is attractive at small separation but becomes repulsive at larger distances $s > 0.5$ nm with barrier 0.1 eV which easily can account for the experimental results in Figs. 1–3.

Although the origin of the long range interaction in graphene may be different from the one in Refs. [18–20] the net effect in the nucleation process is the same: within a shell of size s the repulsive interactions increase the diffusion barrier which in turn reduces the probability of the incoming adatom to diffuse towards the second adatom s lattice constants away. This eventually leads to higher n. In Ref. [24] further investigations were carried out to identify the different contributions to the repulsive barrier, i.e., elastic, dipole-dipole and substrate mediated interactions.

High island densities have been observed in other experimental studies. Regular cluster networks after metal growth on graphene grown on Ir(111) have been reported where nucleation is determined by the Moire pattern formed by graphene and Ir(111) substrate which indicates strong graphene-substrate interaction [26]. Long range electrostatic interactions have been observed during the growth of Au on few-layer graphene (FLG) as a result of charge transfer, limiting the island size for a given graphene thickness [27]. Increasing island density with θ has been observed during growth of Cu on stepped TiO_2 and has been attributed to diffusion barrier modification with increasing θ due to strain [28]. Earlier experiments on inhomogeneous samples where graphene layers coexist with bare buffer layer $6\sqrt{3} \times \sqrt{3}$ have used Co metal atoms as markers to study the conversion form the buffer layer to graphene at higher temperatures [29]. Large differences in island densities were observed with the Co nucleated island density on graphene regions lower by at least a factor of 10 from the density on the $6\sqrt{3} \times \sqrt{3}$ regions, but comparable to the Fe island densities observed in the current experiments.

In summary, very unusual nucleation was found for Fe grown on graphene; both the θ and extremely weak T dependence can be accounted for by long range repulsive interactions. The interaction strength was estimated quantitatively in agreement with DFT calculations. The high Fe island density shows a much richer nucleation behavior and it can have potential applications in magnetic storage technologies. The island density becomes controllable by the deposited amount. The analysis can be quantitatively applied in other systems with similar behavior.

[1] C. Berger, Z. Song, T. Li, X. Li, A. Y. Ogbazghi, R. Feng, Z. Dai, A. N. Marchenkov, E. H. Conrad, P. N. First, and W. A. de Heer, J. Phys. Chem. B **108**, 19 912 (2004).

[2] K. S. Novoselov, A. K. Geim, S. V. Morozov, D. Jiang, Y. Zhang, S. V. Dubonos, I. V. Grigorieva, and A. A. Firsov, Science **306**, 666 (2004).

[3] A. H. Castro Neto, F. Guinea, N. M. R. Peres, K. S. Novoselov, and A. K. Geim, Rev. Mod. Phys. **81**, 109 (2009).

[4] D. L. Miller, K. D. Kubista, G. M. Rutter, M. Ruan, W. A. de Heer, M. Kindermann, P. N. First, and J. A. Stroscio, Nature Phys. **6**, 811 (2010).

[5] J. Wintterlin and M.-L. Bocquet, Surf. Sci. **603**, 1841 (2009).

[6] R. van Gastel, A. T. N'Diaye, D. Wall, J. Coraux, C. Busse, N. M. Buckanie, F.-J. Meyer zu Heringdorf, M.

Horn von Hoegen, T. Michely, and B. Poelsema, Appl. Phys. Lett. **95**, 121901 (2009).

[7] R. Zan, U. Bangert, Q. Ramasse, and K. S. Novoselov, Nano Lett. **11**, 1087 (2011).

[8] S. Barraza-Lopez, M. Vanević, M. Kindermann, and M. Y. Chou, Phys. Rev. Lett. **104**, 076807 (2010).

[9] J. Renard, M. B. Lundeberg, J. A. Folk, and Y. Pennec, Phys. Rev. Lett. **106**, 156101 (2011).

[10] I. Gierz, C. Riedl, U. Starke, C. R. Ast, and K. Kern, Nano Lett. **8**, 4603 (2008).

[11] V. M. Karpan, G. Giovannetti, P. A. Khomyakov, M. Talanana, A. A. Starikov, M. Zwierzycki, J. van den Brink, G. Brocks, and P. J. Kelly, Phys. Rev. Lett. **99**, 176602 (2007).

[12] C. Vo-Van, Z. Kassir-Bodon, H. Yang, J. Coraux, Jan Vogel, S. Pizzini, P. Bayle-Guillemaud, M. Chshiev, L. Ranno, V. Guisset, P. David, V. Salvador, and O. Fruchart, New J. Phys. **12**, 103040 (2010).

[13] D. Fernandez-Torre, D. Fernández-Torre, I. Brihuega, P. Pou, A. J. Martínez-Galera, Rubén Pérez, and J. M. Gómez-Rodríguez, Phys. Rev. Lett. **107**, 116803 (2011).

[14] H. Sevinçli, M. Topsakal, E. Durgun, and S. Ciraci, Phys. Rev. B **77**, 195434 (2008).

[15] J. W. Evans, P. A. Thiel, and M. C. Bartelt, Surf. Sci. Rep. **61**, 1 (2006).

[16] M. Hupalo, S. Binz, and M. C. Tringides, J. Phys. Condens. Matter **23**, 045005 (2011).

[17] M. Hupalo, X. Liu, C.-Z. Wang, W.-C. Lu, Y.-X. Yao, K.-M. Ho, and M. C. Tringides, Adv. Mater. **23**, 2082 2011.

[18] K. Fichthorn and M. Scheffler, Phys. Rev. Lett. **84**, 5371 (2000).

[19] A. Bogicevic, S. Ovesson, P. Hyldgaard, B. I. Lundqvist, H. Brune, and D. R. Jennison, Phys. Rev. Lett. **85**, 1910 (2000).

[20] S. Ovesson, Phys. Rev. Lett. **88**, 116102 (2002).

[21] M. Hupalo, E. H. Conrad, and M. C. Tringides, Phys. Rev. B **80**, 041401(R) (2009).

[22] J. A. Stroscio, D. T. Pierce, and R. A. Dragoset, Phys. Rev. Lett. **70**, 3615 (1993).

[23] J. P. Perdew, K. Burke, and M. Ernzerhof, Phys. Rev. Lett. **77**, 3865 (1996).

[24] X. Liu, C. Z. Wang, M. Hupalo, W.-C. Lu, P. A. Thiel, K. M. Ho, and M. C. Tringides, Phys. Rev. B **84**, 235446 (2011).

[25] T. Olsen, J. Yan, J. J. Mortensen, and K. S. Thygesen, Phys. Rev. Lett. **107**, 156401 (2011).

[26] A. T. N'Diaye, S. Bleikamp, P. J. Feibelman, and T. Micheley, Phys. Rev. Lett. **97**, 215501 (2006).

[27] Z. Luo, L. A. Somers, Y. Dan, T. Ly, N. J. Kybert, E. J. Mele, and A. T. C. Johnson, Nano Lett. **10**, 777 (2010).

[28] D. A. Chen, M. C. Bartelt, and K. F. McCarty, Surf. Sci. **450**, 78 (2000).

[29] S. W. Poon, W. Chen, E. Soon Tok, and A. T. S. Wee, Appl. Phys. Lett. **92**, 104102 (2008).